



## Research article

# Identifying MS4A6A<sup>+</sup> macrophages as potential contributors to the pathogenesis of nonalcoholic fatty liver disease, periodontitis, and type 2 diabetes mellitus

Junhao Wu<sup>a,1</sup>, Jinsheng Wang<sup>b,1</sup>, Caihan Duan<sup>a,1</sup>, Chaoqun Han<sup>a,\*</sup>, Xiaohua Hou<sup>a,\*\*</sup>

<sup>a</sup> Division of Gastroenterology, Union Hospital, Tongji Medical College, Huazhong University of Science and Technology, Wuhan, 430022, China

<sup>b</sup> Department of Gastroenterology, Sir Run Run Shaw Hospital, College of Medicine, Zhejiang University, Hangzhou, Zhejiang, 310016, China

## ARTICLE INFO

## Keywords:

Nonalcoholic fatty liver disease  
Periodontitis  
Type 2 diabetes mellitus  
MS4A6A gene  
Macrophages

## ABSTRACT

**Purpose:** Concrete epidemiological evidence has suggested the mutually-contributing effect respectively between nonalcoholic fatty liver disease (NAFLD), type 2 diabetes mellitus (T2DM), and periodontitis (PD); however, their shared crosstalk mechanism remains an open issue.

**Method:** The NAFLD, PD, and T2DM-related datasets were obtained from the NCBI GEO repository. Their common differentially expressed genes (DEGs) were identified and the functional enrichment analysis performed by the DAVID platform determined relevant biological processes and pathways. Then, the STRING database established a PPI network of such DEGs and topological analysis through Cytoscape 3.7.1 software along with the machine-learning analysis by the least absolute shrinkage and selection operator (LASSO) algorithm screened out hub characteristic genes. Their efficacy was validated by external datasets using the receiver operating characteristic (ROC) curve, and gene expression and location of the most robust one was determined using single-cell sequencing and immunohistochemical staining. Finally, the promising drugs were predicted through the CTD database, and the CB-DOCK 2 and Pymol platform mimicked molecular docking.

**Result:** Intersection of differentially expressed genes from three datasets identified 25 shared DEGs of the three diseases, which were enriched in MHC II-mediated antigen presenting process. PPI network and LASSO machine-learning analysis determined 4 feature genes, of which the MS4A6A gene mainly expressed by macrophages was the hub gene and key immune cell type. Molecular docking simulation chosen fenretinide as the most promising medicant for MS4A6A<sup>+</sup> macrophages.

**Conclusion:** MS4A6A<sup>+</sup> macrophages were suggested to be important immune-related mediators in the progression of NAFLD, PD, and T2DM pathologies.

\* Corresponding author. Division of Gastroenterology, Union Hospital, Tongji Medical College, Huazhong University of Science and Technology, 1277 Jiefang Avenue, Wuhan, Hubei Province, 430022, China.

\*\* Corresponding author. Division of Gastroenterology, Union Hospital of Tongji Medical College, Huazhong University of Science and Technology, 1277 Jiefang Avenue, Wuhan, Hubei Province, 430022, China.

E-mail addresses: [hcq1987912@hotmail.com](mailto:hcq1987912@hotmail.com) (C. Han), [houxh@hust.edu.cn](mailto:houxh@hust.edu.cn) (X. Hou).

<sup>1</sup> These authors contributed equally to this work and shared the first authorship.

<https://doi.org/10.1016/j.heliyon.2024.e29340>

Received 18 January 2024; Received in revised form 14 March 2024; Accepted 5 April 2024

Available online 9 April 2024

2405-8440/© 2024 The Authors. Published by Elsevier Ltd. This is an open access article under the CC BY-NC-ND license (<http://creativecommons.org/licenses/by-nc-nd/4.0/>).

## 1. Introduction

Periodontitis (PD) is an oral disease which can result in the loss of tooth support tissues and eventually teeth that may be attributed to anaerobic gram-negative bacteria-mediated microbial imbalance (chiefly the *Porphyromonas gingivalis*) and subsequent host immune reactions [1,2]. Globally, it is estimated that up to 3.5 billion people (nearly half of the world's population) have PD, and 1.1 billion have severe degree, according to the Global Burden of Disease (GBD) Study 2019 [3]. Moreover, elevated circulating exotoxins, inflammatory cytokines, reactive oxygen species along with bacteremia that potentially originate from inflamed periodontal soft tissues could enhance the susceptibility to and aggravate systemic disease, including type 2 diabetes mellitus (T2DM) and, in particular, nonalcoholic fatty liver disease (NAFLD) [4–6], as

indicated by numerous epidemiological [7–9], experimental [10], and clinical works [11,12]. Long-lasting antibiotic use, however, cannot effectively remove dental plaques or calculus, and mechanical debridement might fail to diminish pathogens residing in the non-dental biofilms (e.g., tongue mucosa, oral mucosa), ultimately leading to gingival recession or dentin hypersensitivity [13].

Being the most common metabolic disorder characterized by hyper-glycemia and insulin resistance [14], T2DM now affects more than 0.5 billion people worldwide and

this count would reach 1.31 billion by 2050 if measures against T2DM were not taken.

[15]. The potent link between PD and T2DM lies in that PD is not only an established risk factor for (resulting in insulin resistance and dysregulated blood glucose control), but also a complication of (contributing to the disruption of teeth supporting structures) diabetes [16,17]. Moreover, T2DM is thought to accelerate NAFLD development, and

therefore, the prevalence of NAFLD is higher in patients with T2DM (about one-third have steatohepatitis) [18–21]. These results indicate a mutually detrimental correlation between T2DM and NAFLD [18].

NAFLD refers to a pathologic liver status accompanied by excessive fat deposits

in at least 5 % of hepatocytes in individuals without alcoholism or the secondary cause

of hepatic steatosis, which is reported to affect 26.8 % of the population worldwide [22–24], and the morbidity from relevant diseases until 2030 would double than that of today [25]. The pathology of NAFLD ranges from simple steatosis to more severe nonalcoholic steatohepatitis (NASH) that would finally deteriorate into end-stage liver disease, including liver cirrhosis and hepatocellular carcinoma [26]. It has been estimated that as many as 30 % of NAFLD patients suffer from NASH [27]. In turn, increased prevalence and severe degrees of PD are indicated in NAFLD patients [6,28,29], and PD-related *Porphyromonas gingivalis* is more frequently detected in saliva tissues of NAFLD patients [30]. Furthermore, 47.3–63.7 % of T2DM

patients were accompanied by NAFLD as insulin resistance-caused lipolysis results in liver fatty acid accumulation, which overwhelms the organic metabolism capacity and forms lipotoxic burden to mediate hepatocellular injuries and apoptosis [31,32].

Prior studies provide preliminary evidence supporting potential linkages between.

NAFLD and PD, NAFLD and T2DM, along with PD and T2DM respectively, through abundant *in vitro/in vivo* experiments [33–35]. The inter-organ crosstalk, which refers to interactions between organs and tissues upon pathophysiological situations through

secreted exosomes (containing proteins, lipids and small noncoding RNAs), circulated proteins, lipids and even certain metabolites in an endocrine/paracrine way, has been widely investigated as an important pathway to learn about their pathogenesis [36,37]. Nevertheless, the specific characteristics of dysregulated immune cells associated with NAFLD, T2DM, and PD remain unresolved. Recently, the rapid development of high-throughput RNA sequencing technologies and bioinformatic analyses methods facilitate deeper insights into the pathogenesis from a transcriptomic level of human samples rather than animal or cell samples [38]. Furthermore, machine-learning algorithms help screen out features biomarkers along with single-cell RNA sequencing technique contributed to early and accurate detection/validation of specific cell phenotypes in complicated pathologies [39]. Given that upon chronic inflammatory status, circulating monocytes may infiltrate and accumulate in inflamed

tissue sites to initiate or even aggravate disease severity [40], we assumed that this cell type could also play a significant role in PD-NAFLD-T2DM conditions.

## 2. Materials and methods

### 2.1. Data collection and preprocessing

As of October 2023, the Gene Expression Omnibus (GEO) database (<https://www.ncbi.nlm.nih.gov/geo>) was searched using keywords: “periodontitis”, “nonalcoholic fatty liver disease” to acquire targeted microarray datasets [41]. For PD, the GSE10334, and GSE16134 datasets were chosen for data mining and data validation, respectively. For NAFLD, the GSE164760 and GSE63067 datasets were chosen. Moreover, T2DM-related datasets were downloaded from the GSE76895 and GSE76894 datasets of non-diabetic or not islets. Then, each probe was matched with and replaced by one specific gene symbol using the platform annotated files and if multiple probes corresponded to one gene in a sample, the averages of the expression values were adopted. Probe sets without corresponding gene symbols were removed. The array data expression matrix was normalized by robust multichip average (RMA) when necessary. The output gene matrix consisted of rows named as gene symbols and columns named as sample serial numbers.

From the above datasets, the PD and healthy samples were collected based on the

defined instructions. The NASH samples are acquired from individuals of the NAFLD datasets with a definite diagnosis of NASH. In

T2DM, we selected pancreatic islet from human donors. All datasets used in this study belong to “*Homo sapiens*” and their details are listed in Table 1.

## 2.2. Differentially expressed genes (DEGs) analysis

With  $P$  value  $< 0.05$  and “Foldchange”  $> “1.2”$ , the DEGs were recognized by the.

“Limma” algorithm in PD-related GSE10334 and GSE16134 dataset; NAFLD-related GSE164760, GSE63067 dataset along with T2DM-related GSE76895 and GSE76894

dataset. Then the results of these datasets were intersected to acquire the shared DEGs of these three diseases. The “ggplot” R package depicted DEGs in volcano plots along

with the “pheatmap” R package visualized changes in the expression values of the top.

Fifty genes in different samples by heatmaps [42,43].

## 2.3. Functional and pathway enrichment analysis

Functional enrichment analysis was performed via using the DAVID (version 6.8, <https://david.ncifcrf.gov/>) database, which provides a deeper and more comprehensive understanding of the biological functions and pathways implicated by cross-talk genes.

The Gene Ontology (GO) enrichment analysis includes three parts: Biological Process: (BP), Molecular Function: (MF), Cellular Component: (CC). The Kyoto Encyclopedia

of Genes and Genomes (KEGG) and REACTOME pathway enrichment analysis were

used to identify all pathways.  $P$  value  $< 0.05$  is set as the cutoff value.

## 2.4. Protein-protein interaction (PPI) network construction, hub module and gene identification

The DEGs were imported into the STRING database (<http://www.string-db.org/>):

to build a PPI network, presenting direct and indirect protein-protein interactions. The minimum combined score  $\geq 0.4$  was chosen to build a PPI network and the Cytoscape software (version 3.7.1) visualized the result. Topological analysis of the network was analyzed by the maximal clique centrality (MCC) algorithm of the CytoHubba plug-in and the CytoNCA plug-in of Cytoscape [44]. The shared top 10 DEGs were thought to be the most important genes for constructing the hub cluster network.

## 2.5. Identification of hub cross-talk genes by machine-learning analysis

To identify hub feature genes shared by the diseases, the least absolute shrinkage

and selection operator (LASSO) algorithm was utilized [45], which was characterized by penalty regression that can identify feature genes from high-dimensional data with the “cv.glmnet” function of the “glmnet” R package, with a minimal lambda as optimal [46]. The penalized term was selected by 10-fold cross-validation. This algorithm evaluated the strongest association with outcomes in various factors without being influenced by confounding factors [47]. In addition, to examine the diagnostic and discriminative value of the genes, the receiver operating characteristic (ROC) curves were established with the area under the ROC curve (AUC) being assessed.

## 2.6. Single-cell RNA sequencing data and immunohistochemical analysis

The immunohistochemical slices data of the MS4A6A protein in multiple organs were obtained from the human protein atlas (HPA)

**Table 1**

Detailed information of PD, NAFLD, and T2DM-related datasets.

Disease	ID	Dataset num.	Source	Platform	Case	Control
NAFLD	1	GSE164760	liver tissues	GPL13667	n = 74	n = 6
	2	GSE63067	liver tissues	GPL570	n = 9	n = 7
T2DM	1	GSE76894	pancreas islets	GPL570	n = 19	n = 84
	2	GSE76895	pancreas islets	GPL570	n = 36	n = 32
PD	1	GSE10334	gingival tissues	GPL570	n = 183	n = 64
	2	GSE16134	gingival tissues	GPL570	n = 241	n = 69

<sup>a</sup>PD, periodontitis; NAFLD, nonalcoholic fatty liver disease; T2DM, type 2 diabetes mellitus; num., number. All RNA-sequencing data used in this study were acquired from human samples.

**Table 2**  
DEGs of PD, NAFLD, and T2DM-related datasets.

Up-regulated genes	Down-regulated genes
20 genes CYTIP/PLAC8/LY96/FCER1G/LAPTM5/PTPRC/HLA-DMA/C1orf162/HLA-DMB/TLR1/CYP1B1/PPP1R3B/MS4A6A/MS4A7/IKZF1/TSPAN12/MAMDC4/ANGPT2/KCNAB2/PIK3R5	5 genes STARD10/MBNL1-AS1/PTPN3/LACTB2/SERTAD4

<sup>a</sup>DEGs, differentially expressed genes; NAFLD, nonalcoholic fatty liver disease; PD, periodontitis; T2DM, type 2 diabetes mellitus.

**Table 3**  
Molecular docking simulation results.

Molecules	Binding energy	Binding amino acid residue
Fenretinide	-6.9 kcal/mol	ALA67 SER80 LEU83 ASN84 ALA86 PHE89 ILE90 PHE93 PHE94
Sulforaphane	-3.6 kcal/mol	ASP35 LYS38 LYS39 LEU41 HIS42 ILE45 SER102 THR105 GLU106 LEU109 ARG207 GLN210
Taurine	-3.6 kcal/mol	LEU41 HIS42 ILE45 SER102 THR105 GLU106 LEU109 ARG207 GLN210 ASP214

database (<https://www.proteinatlas.org/>). Single-cell RNA sequencing analysis of the MS4A6A gene was performed the DISCO database (<https://www.immunesinglecell.org/>) [48], providing MS4A6A gene expression data of in various tissues from single-cell level. The cell cluster results were displayed using uniform manifold approximation and projection (UMAP). The annotation of the specific cell types relied on the expression of known canonical markers.

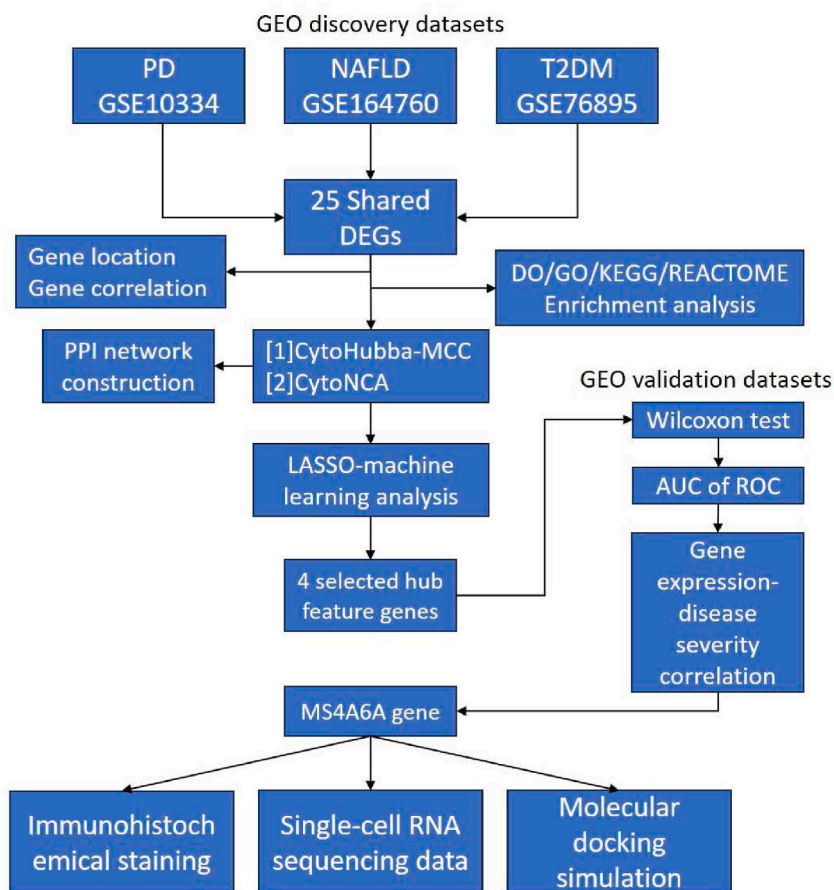
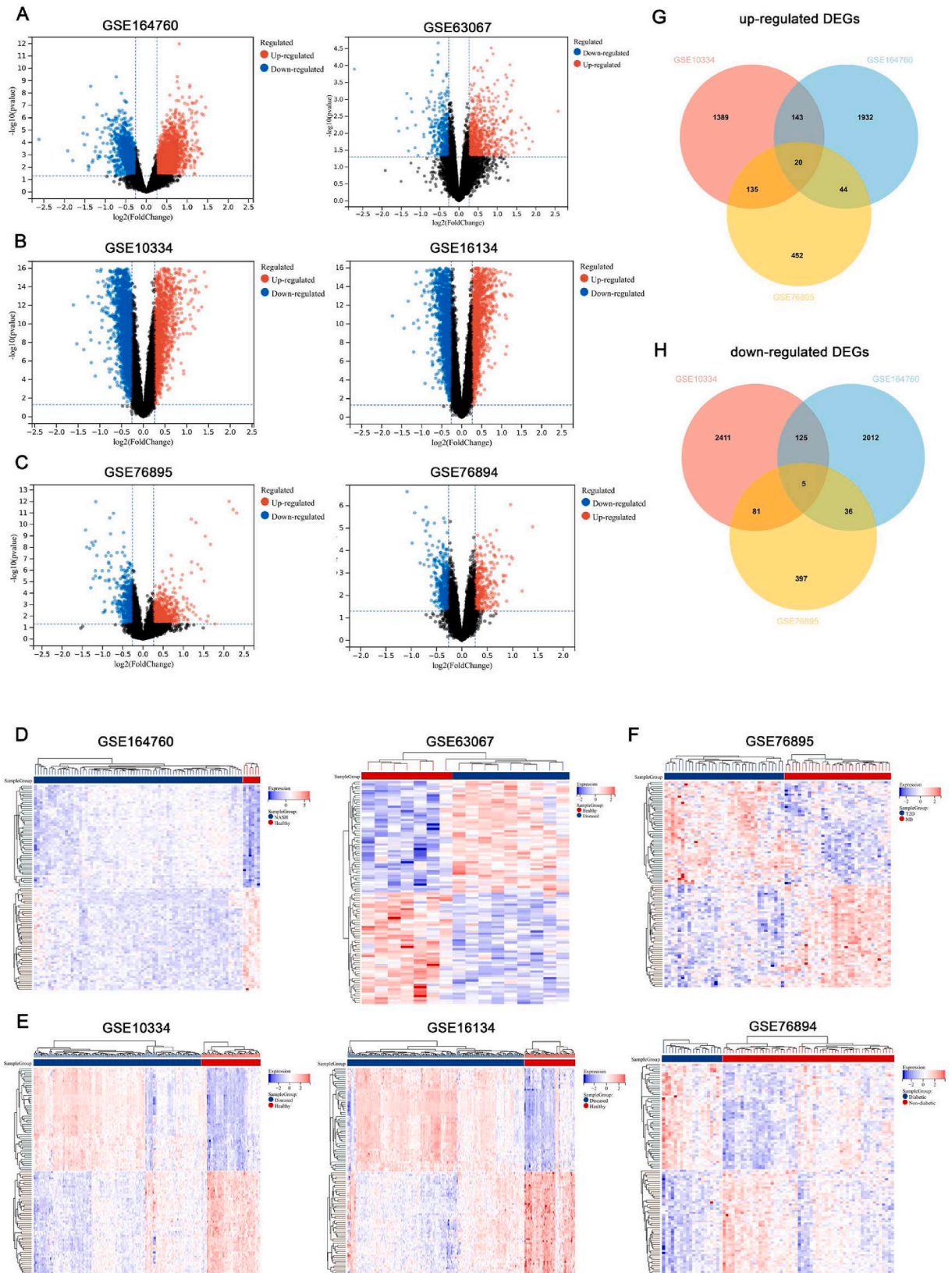


**Fig. 1.** The flowchart of the study design

\*PD, periodontitis; NAFLD, nonalcoholic fatty liver disease; T2DM, type 2 diabetes mellitus; DEGs, differentially expressed genes; LASSO, least absolute shrinkage and selection operator; ROC, receiver operating characteristic curve.



(caption on next page)

**Fig. 2.** Identification of DEGs in PD, NAFLD, and T2DM-related datasets

(A) Gene expression profiles in NAFLD-related GSE63067 and GSE164760 datasets. (B) Gene expression profiles in PD-related GSE10334 and GSE16134 datasets. (C) Gene expression profiles in T2DM-related GSE76894 and GSE76895 datasets. (D) Heatmaps showing the top fifty DEGs in the GSE63067 and GSE164760 datasets. (E) Heatmaps of the top fifty DEGs in the GSE10334 and GSE16134 datasets. (F) The heatmaps of the top fifty DEGs in the GSE76894 and GSE76895 datasets. (G) A Venn diagram showing 20 shared upregulated DEGs by GSE76895, GSE10334, and GSE164760 datasets. (H) A Venny diagram exhibiting 5 shared downregulated DEGs by GSE76895, GSE10334, and GSE164760 datasets. In A-C, the X-axis refers to  $\log_2$  |Foldchange| and the Y-axis represents  $-\log_{10}(p \text{ value})$ . The blue and red dots represent downregulated and upregulated DEGs, respectively. In D-F, the diagrams showing the results of a Two-way hierarchical clustering of all samples and the top fifty DEGs in each dataset. PD, periodontitis; NAFLD, nonalcoholic fatty liver disease; T2DM, type 2 diabetes mellitus; DEGs, differentially expressed genes.

### 2.7. Molecular docking simulation

The Comparative Toxicogenomics Database (CTD; <https://ctdbase.org/>) of Gene-Drug interaction data were used to predict potential therapeutic drugs. The PDB structure file of the MS4A6A protein was downloaded from AlphaFold Protein Structure Database (<https://alphafold.ebi.ac.uk/>). The sdf structure file of those predicted small therapeutic molecules was acquired from the PubChem database. The molecular docking simulation was finished using CB-DOCK2 database for automated protein-ligand blind docking [49]. Finally, the Ligplot and PyMOL software visualized the intermolecular binding patterns in two-dimensional and three-dimensional graphs, respectively.

### 2.8. Statistical analysis

R software version 4.2.1, GraphPad Prism version 9.4.0 (GraphPad Software, San Diego, CA, USA), and SPSS Version 26.0 (IBM Corporation, Armonk, NY, USA) were adopted to perform statistical analysis. The differences between the groups were tested using Wilcoxon's test ( $P \text{ value} < 0.05$ ). The spearman's method was adopted to analyze correlation between the core genes and immune cells. In addition, the receiver operating characteristic (ROC) curves were analyzed using the "pROC" R package. The significance level is denoted by \* $P \text{ value} < 0.05$ , \*\* $P \text{ value} < 0.01$ , \*\*\* $P \text{ value} < 0.001$ , and \*\*\*\* $P \text{ value} < 0.0001$ .

The workflow chart (Fig. 1) depicts the overall study design.

## 3. Results

### 3.1. Identification of shared DEGs of PD, NAFLD, and T2DM

The differential analysis screened out 4317 DEGs, including 2139 up-regulated.

DEGs and 2178 down-regulated DEGs related to NAFLD, in the GSE164760 dataset. In addition, a total of 808 up-regulated with 383 down-regulated DEGs were screened

out in the GSE63067 dataset. For PD, the differential analysis identified totally 1687 up-regulated DEGs and 2622 down-regulated DEGs in the GSE10334 dataset, along with 1822 up-regulated and 2067 down-regulated DEGs in the GSE16134 dataset. Moreover, there were 1170 T2DM-related DEGs including 651 up-regulated and 519 down-regulated in the GSE76895 dataset, along with 2322 genes in the GSE7689. 4 dataset. The volcano plots (Fig. 2A-C) exhibit the gene expression patterns of the NAFLD, PD, and T2DM-related datasets and the heatmaps (Fig. 2D-F) display the distribution patterns of the most prominent DEGs. The Venny diagrams (Fig. 2G-H) intersect a total of 20 up-regulated and 5 down-regulated genes in the above discovery datasets regarding to these three pathologies (Table 2).

### 3.2. Functional enrichment analysis

To reveal potential biological functions of the above shared DEGs, we performed. DO, GO, KEGG, and REACTOME enrichment analysis. The DO result demonstrated the correlations with "periodontal disease", "primary bacterial infectious disease", and "diabetes mellitus" (Fig. 3A). In addition, GO analysis showed enriched biological process (BP), cellular component (CC), and molecular function (MF) terms regarding:

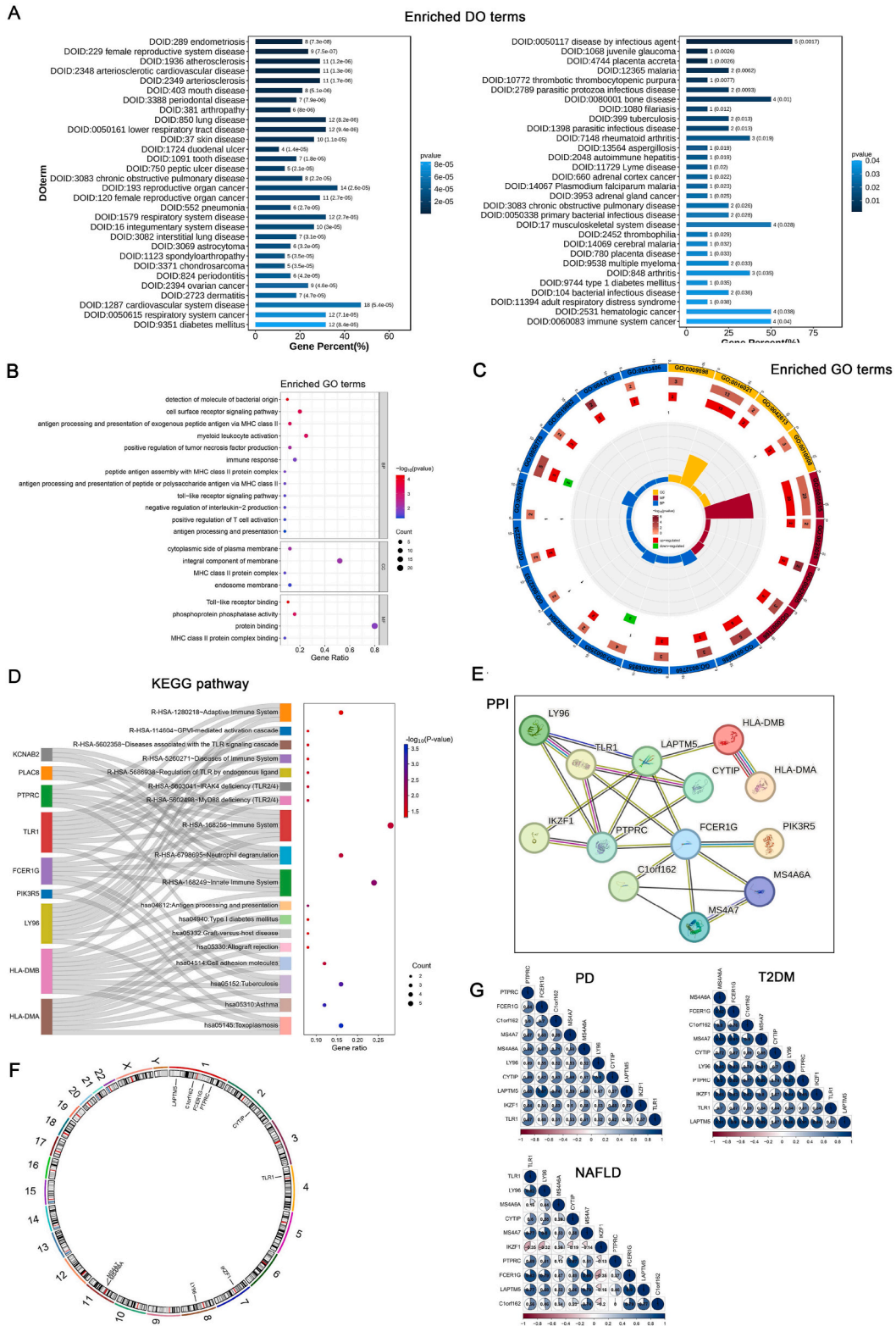


**Fig. 3.** Functional enrichment analysis of these DEGs (A) DO analysis results of the 25 shared DEGs. (B) GO analysis results of the 25 shared DEGs, including terms of biological process (BP), molecular function (MF) and cellular component (CC). (C) The enriched GO terms of BP, CC, and MF, as shown in the circular diagram. (D) The KEGG and REACTOME pathway enrichment analyses results. (E) The PPI network of 25

shared DEGs built by the STRING database, which displayed the connections between 13 genes, with the threshold set as  $> 0.400$  (F) The Circos track plot showing the locations of the hub module genes on chromosomes. (G) The correlations of the 13 genes in PD, NAFLD, and T2DM. The blue color indicates a positive correlation and the red color indicates the opposite. DEGs, differentially expressed genes; PD, periodontitis; NAFLD, nonalcoholic fatty liver disease; T2DM, type 2 diabetes mellitus.

“positive regulation of tumor necrosis factor production”, “toll-like receptor signaling pathway”, “MHC class II protein complex assembly”, “myeloid leukocyte activation”, “antigen processing and presentation of exogenous peptide antigen via MHC class II”, and “antigen processing and presentation of peptide or polysaccharide antigen via MHC class II” for BP, “MHC class II protein complex” for CC, along with “MHC class II protein complex binding” and “toll-like receptor binding” for MF (Fig. 3B-C). The KEGG and REACTOME pathway enrichment analyses demonstrated the involvement of “antigen processing and presentation”, “diseases associated with the TLR signaling cascade”, and TLR2/4 signaling-related pathways (Fig. 3D). Such results indicated the prominent enrichment of various immuno-inflammatory pathways, particularly the MHC class II protein-mediated antigen processing/presentation pathway, and Toll-like (TLR) signaling pathways. These findings demonstrated that their underlying linkages were primarily caused by immunological responses.

### 3.3. PPI network construction and hub gene identification

The PPI network was built to show interactions between DEGs (Fig. 3E), and Cytoscape 3.7.1 was used for visualization. The “MCC” algorithm of the CytoHubba plugin and the CytoNCA plugin of Cytoscape 3.7.1 selected out potentially significant cross-talk genes, such as MS4A6A, MS4A7, and C1orf162 (Fig. 4A). These shared genes were expressed by dendritic cells (red color), or immune organs, including bone marrow (blue color) and spleen (green color) that answered for generating and storing immune cells (Fig. 4B). In addition, in Fig. 3F the Circos track plot showed the location of such shared genes on chromosomes, which provided insights into potential intersected genetic regions of these three diseases. The coloring scheme indicated the the majority of positive correlations among the 10 shared genes as for their expression levels, with blue indicating positive correlations and red indicating the opposite trend (Fig. 3G).

### 3.4. Selecting characteristic genes through machine-learning analysis

The LASSO-Cox machine learning algorithm was adopted to screen out potential feature genes shared by NAFLD, T2DM, and PD. The results are depicted in Fig. 4 C, with the overlapping genes listed as LY96, TLR1, CYTIP, and MS4A6A. Besides, Fig. 4D prominently demonstrates a higher expression level of such 4 hub genes in upon diseased conditions than in healthy people. Subsequently, the diagnostic efficacy of these biomarkers was analyzed, and the ROC curves showed that the area under the curve (AUC) of LY96, TLR1, CYTIP, and MS4A6A in discovery datasets Fig. 5A, respectively. We validated the results in external datasets GSE16134 (PD), GSE63067. (NAFLD), and GSE76894 (T2DM) (Fig. 5B). However, the ROC curves indicated that TLR1 and LY96 had the lowest discriminatory powers in NAFLD (AUC = 0.606) and T2DM (AUC = 0.555), possibly attributed to their not being prominently different levels in distinct groups. The CYTIP gene was not matched in the other T2DM dataset. Therefore, the MS4A6A gene was deemed as the most important characteristic marker upon the pathologies simultaneously. More importantly, further analysis demonstrated that MS4A6A mRNA expression level was positively associated with: Fasting glucose levels in T2DM patients; NAS score of NAFLD patients; Pro-inflammatory cytokines. (i.e., CXCL8) levels in PD patients (Fig. 5C), meaning that MS4A6A mRNA level was positively associated with the severity of PD, NAFLD, and T2DM. Overall, these 4 hub genes were mainly enriched in macrophages, supporting their great significance in disease progression. In addition, the expression of the MS4A6A gene in gingival, liver, and pancreatic tissues were analyzed by immunohistochemical staining as well as its cellular location by single-cell RNA sequencing analysis. As demonstrated in Fig. 6A-B; Fig. S1, the expression of MS4A6A in these tissues was largely by macrophages.

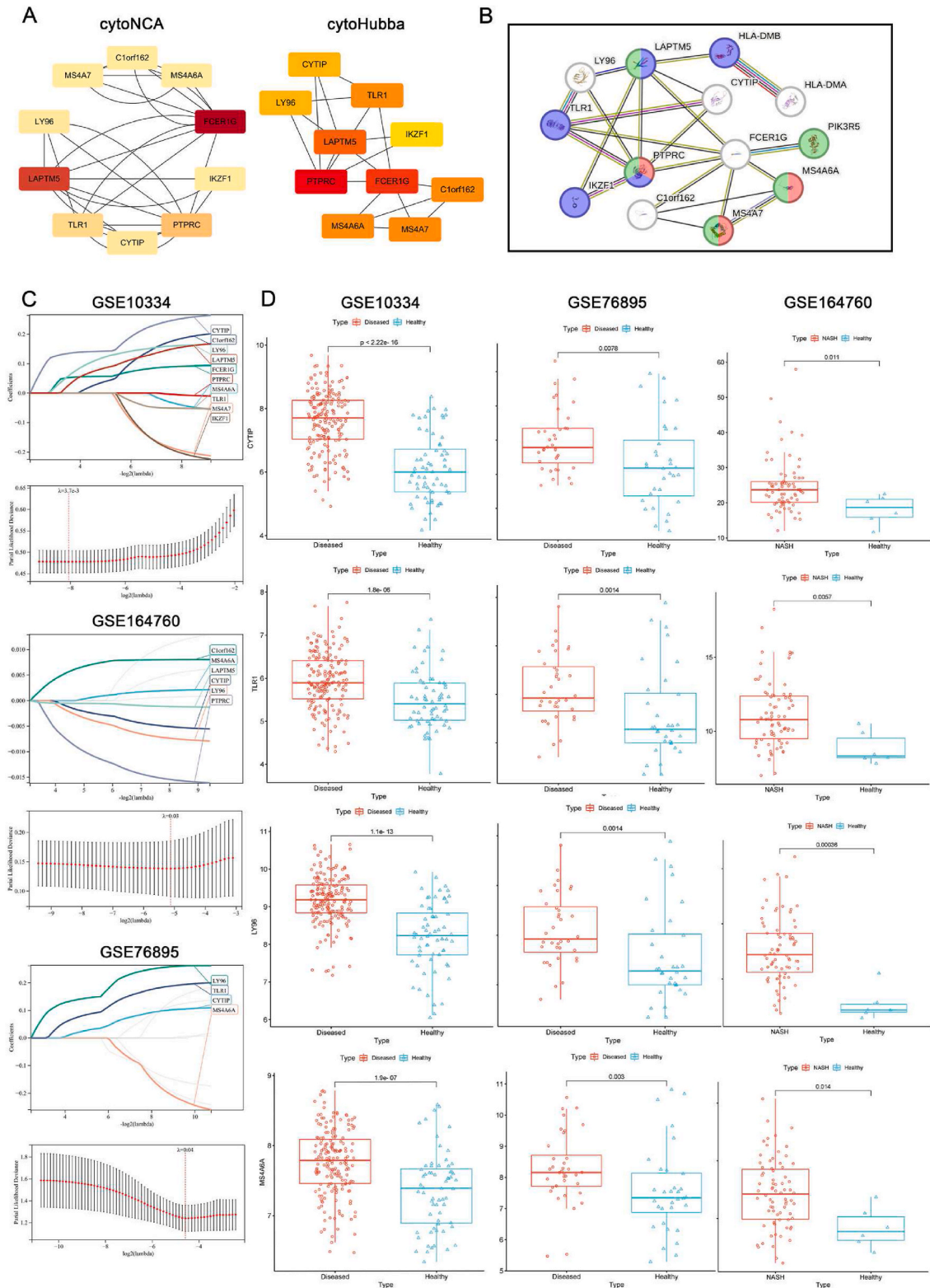


**Fig. 4.** Identifying hub feature genes via the LASSO machine-learning algorithm (A) Hub modules of the PPI network selected by the cytoNCA and MCC algorithm of the cytoHubba plugins of Cytoscape software 3.7.1. Both modules contain the same 10 genes. (B) Predictions of gene expression locations of the 13 genes in the

PPI network. Red indicates the expression by antigen-presenting cells; Blue refers to expression by bone marrow; Green indicates expression by the spleen. (C) Identification of the key feature genes of PD, NAFLD, and T2DM by the LASSO machine-learning algorithm. (D) Boxplots comparing the expression levels of these 4 preliminarily identified hub feature genes shared by PD, NAFLD, and T2DM, which showed lower expression levels of these 4 genes in pathologies in comparison to in healthy status. PD, periodontitis; NAFLD, nonalcoholic fatty liver disease; T2DM, type 2 diabetes mellitus; LASSO, least absolute shrinkage and selection operator.

### 3.5. Predicting therapeutic agents and molecular docking simulation

The CTD database predicted correlations between the MS4A6A gene and disease, demonstrating its close association with glucose dysregulation, liver lipid metabolism abnormalities, and gingival inflammation (Fig. S2). In addition, the CTD database predicted potential therapeutic agents, including astemizole, fenretinide, gardiquimod, oxaliplatin, sulforaphane, taurine, and topotecan. Given that astemizole may well lead to severe cardiovascular side effects, oxaliplatin and topotecan were chemotherapeutic agents not fitting for daily use in noncancer patients, and that gardiquimod was not in the market, fenretinide, sulforaphane, and taurine were chosen as potential therapeutic small molecules (Figure.S3; Table 3).

We then performed a molecular docking simulation, and the results suggested an intimate binding between MS4A6A and fenretinide at a binding score of  $-6.9$  kcal/mol. The molecular structures of fenretinide and MS4A6A were visualized in cartoon form, with corresponding 2D graphs showing hydrophobic contacts between fenretinide and six amino acid residues (Phe89, Asn84, Leu83, Phe93, Phe94, and Ile90) of MS4A6A, and with 3D graphs indicating hydrogen-bond interactions by yellow dotted lines. The same process was also carried out regarding to sulforaphane and taurine whereas their intermolecular binding capacity was not as good. Therefore, fenretinide was chosen to be the most promising small molecule for therapy based on molecular docking results, which supported its relatively-intimate binding with the MS4A6A protein (Fig. 7).

## 4. Discussion

Our study for the first time used systemic biological methods to indicate MS4A6A<sup>+</sup> macrophages as a potentially-shared immunological therapy target under PD, NAFLD, and T2DM pathologies. Currently, the unprecedentedly-high prevalence of metabolic syndrome has led to heavy social burden and economic loss globally [50], and therefore calls for more efforts to investigate their potential connections. Recent advances in characterizing molecular and cellular heterogeneity from a single-cell level helps us better understand activities of immune-related genes/cells in chronic inflammatory pathologies.

Chronic inflammation is a main feature of PD, NAFLD, and T2DM [51]. Correlated subclinical endotoxemia along with activated mononuclear cells (including an array of antigen-presenting cells, e.g., macrophages) in circulation that progressively migrated into the affected sites have been proven to underlie such pathologies [52]. As a main type of innate immune cells, resident macrophages and peripheral monocyte-derived ones recruited from circulation are critical to deteriorating or eliminating infection [53]. The activated macrophages are divided into the contradictory M1 (proinflammatory), and M2 (immune-modulatory) subtypes on the basis of their cell surface biomarkers [54]. GO and KEGG/REACTOME analyses highly enriched MHC-II-mediated antigen processing/presentation process, which could then trigger T lymphocytes activation via stimulating T cell receptors [55]. T cell activation is a significant process in such transition from acute inflammatory response to chronic inflammation [56], which is exactly the condition of these three pathologies.

Also, trajectory analysis of single-cell RNA sequencing data further demonstrated that the proliferative differentiation of macrophages originated from the MHC-II clusters and expressed more genes for antigen processing and presentation [57]. In the present work, we recognized the MS4A6A gene as the final potential biomarker of the disease development after rigorous filtration and validation by external datasets. MS4A6A belongs to the human MS4A family, of which the 18 members are encoded by a genomic locus on chromosome 11q12, and differentially expressed by specific subsets of leukocytes [58]. In *Homo sapiens*, MS4A6A is specifically enriched in monocytes and macrophages at high levels, particularly in alternatively activated macrophages where they cooperate with the protein partner MS4A4A to regulate the activities of pattern recognition receptors in type I immunity, as a classical monocyte-specific cluster of MS4A proteins [59]. Other evidence indicated that macrophages rather than dendritic cells solely express MS4A6A in human beings [60]. In microglia (which is a population of central nervous system (CNS)-resident macrophages [61]), MS4A6A is an important gene for immune activation, which demonstrated enhanced chromatin accessibility of a distal open chromatin region along with increased transcription upon infectious stimulation or increased risk of Alzheimer's disease [62,63]. In hypersensitivity pneumonitis, the high MS4A6A<sup>+</sup> subgroup was significantly infiltrated and contributed to severe fibrotic progression, which displayed more M1 and M2 macrophages signature genes along with exaggerated inflammatory response signatures compared to others [64], such as inducing myeloid leukocyte migration and attracting chemotaxis infiltration [65]. Such a seemingly contradictory positive association between M1 and M2 polarization markers expression level as well as a mixed state of M1 and M2 phenotypes at single-cell level of macrophages was increasingly validated [66,67], indicating that conventional classification of macrophages into

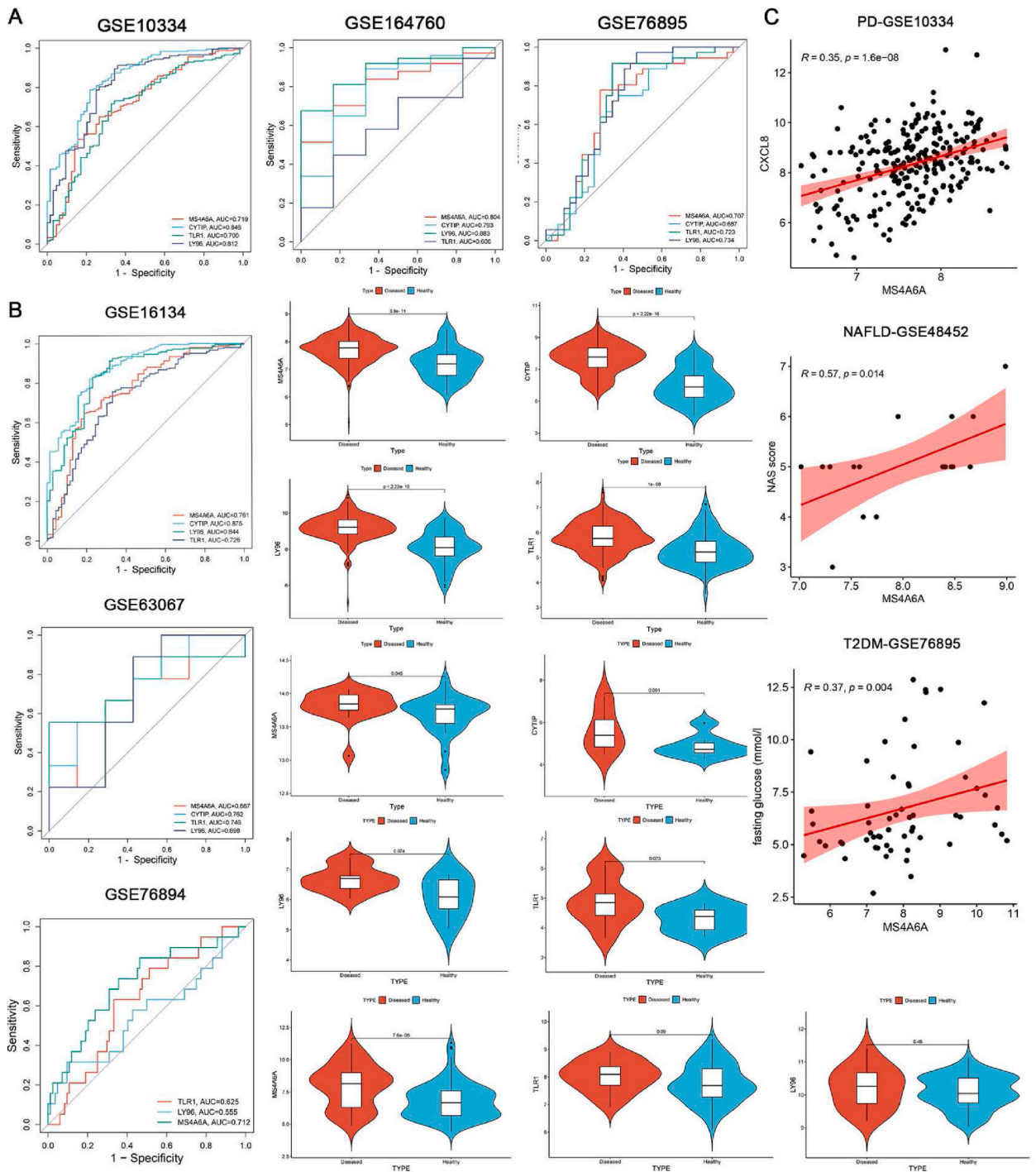


**Fig. 5.** Validation of the efficacy of 4 hub feature genes

(A) The ROC curves showing the diagnostic efficacy of these 4 genes in GSE164760, GSE10334, and GSE76895 datasets. (B) The ROC curves and violin plots showing the diagnostic efficacy and the expression level of the hub feature genes in GSE63067, GSE16134, and GSE76894 datasets, except for the CYTIP gene that is not matched in the GSE76894 validation dataset. (C) The correlations between the expression level of the MS4A6A gene and disease severity markers of PD, NAFLD, and T2DM. (CXCL8 for PD; NAS score for NAFLD; fasting glucose level for T2DM). PD, periodontitis; NAFLD, nonalcoholic fatty liver disease; T2DM, type 2 diabetes.

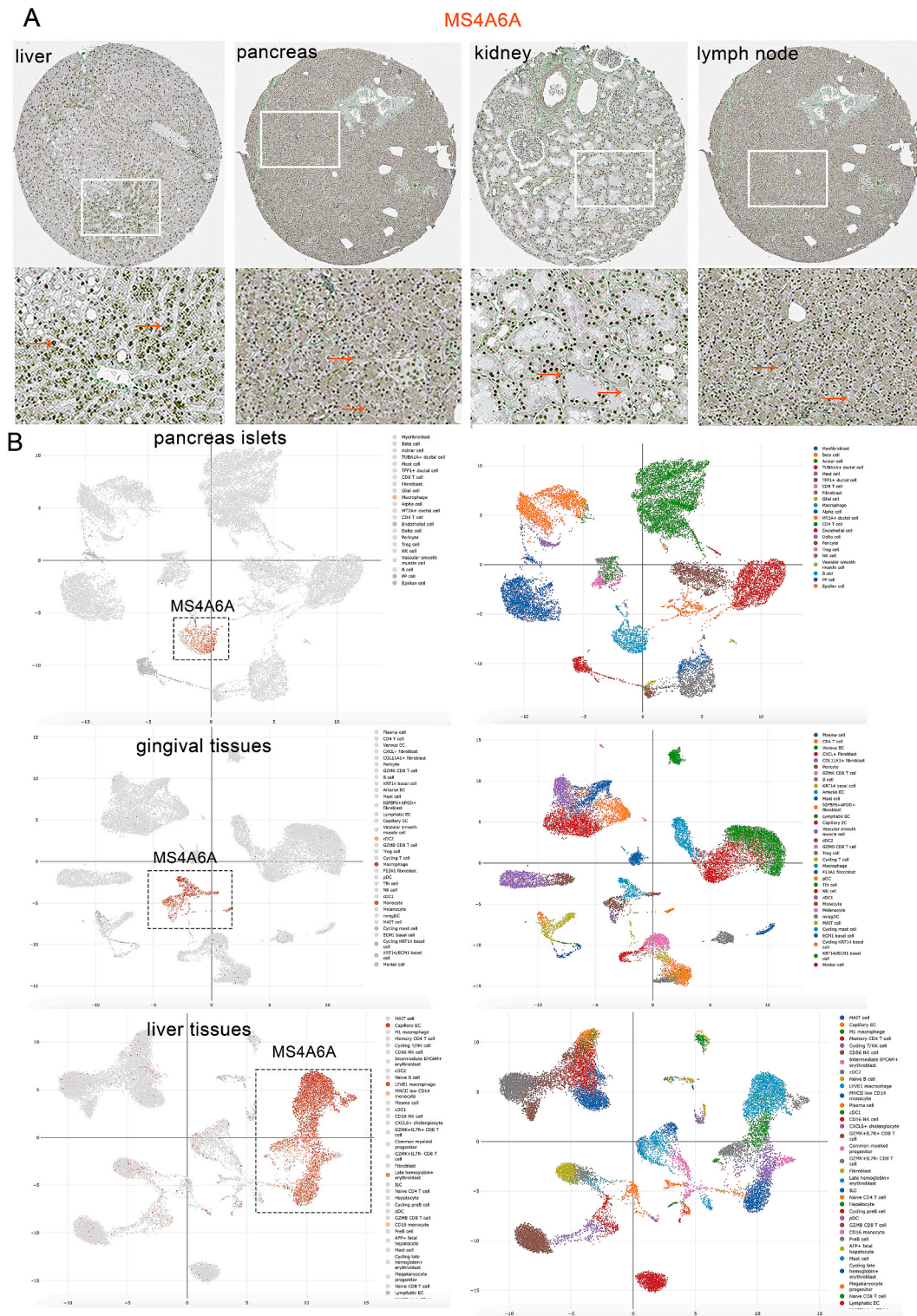


**Fig. 6.** Single-cell analysis and immunohistochemical staining data (A) Immunohistochemical staining graphs of the MS4A6A gene in various tissues. The graphs were acquired from the HPA database (<https://www.proteinatlas.org/>). Red arrows below indicate the expression site and level of the MS4A6A gene. (B) The single-cell RNA sequencing analysis showing cell types expressing the MS4A6A gene in PD, NAFLD, and T2DM. The results suggested a high and unique expression of the

MS4A6A gene in macrophages. The orange color refers to its expression level and the darker the orange color is, the higher expression level of the MS4A6A gene. NAFLD, nonalcoholic fatty liver disease; T2DM, type 2 diabetes mellitus; PD, periodontitis.

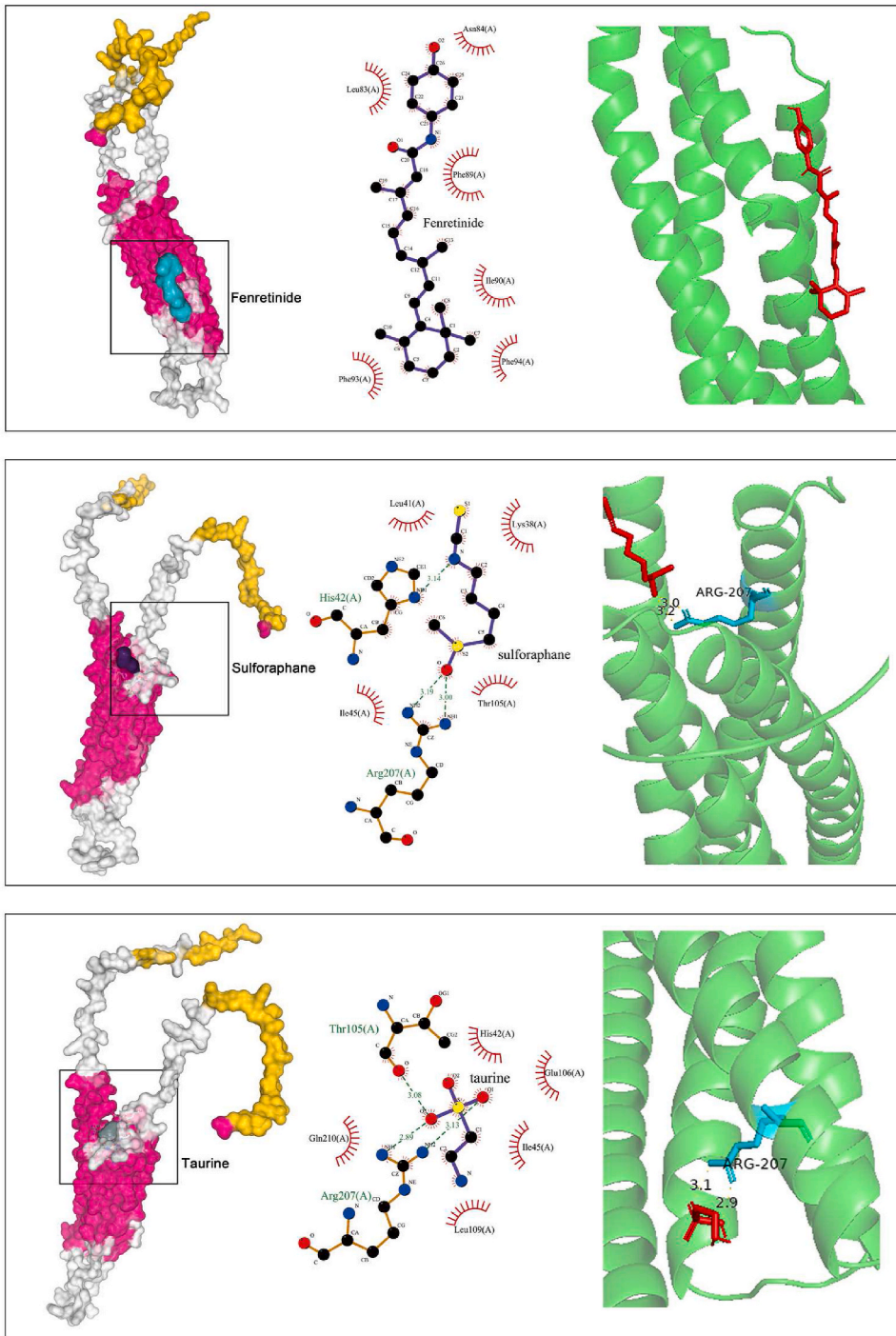


**Fig. 7.** Intermolecular docking simulation results of the predicted drugs with MS4A6A protein.

mutually-exclusive M1/M2 phenotypes was unable to reflect their broad variations and continuous spectrum of transcriptomic status upon dynamically complicated disease conditions [68]. Therefore, increased MS4A6A gene expression in macrophages might be one of the most significant factors governing such transition in tissue inflammation status.

As for PD, M1-type macrophages migrate to sites of acute inflammatory through diapedesis to generate pro-inflammatory cytokines in the early phase [69], while a higher level of accumulated and activated M2-phenotype macrophages was detected in chronic and severe inflammation [70,71]. Such enhanced M2-phenotypes of macrophages also detected in inflammation rather than resolution phases of PD may be attributed to impaired immune response due to obesity (obesity is largely found in NAFLD/T2DM patients as discussed before) [52], which could inhibit the polarization of macrophages to the M1-phenotype that have an enhanced ability to eliminate pathogens and infections, and the resultant increased M2-phenotype macrophages led to a delayed and impaired response to periodontal infections [72]. Our results indicated a simultaneous upregulation of both M2-type and M1-type macrophages in the PD microenvironment, which could be accounted for by the above-discussed mechanism, mechanical force's regulation of macrophages in the tissue remodeling stage, and continuous phenotype alteration of M1/M2-type macrophages that were not mutually-exclusive [52,73]. This assumption was supported by the other work using non-human primate models and found changes in gene expression profiles for M2 macrophages in

addition to substantial M1 polarization-related gene expression alterations [74]. Single-cell sequencing analysis also indicated upregulated pro-inflammatory and anti-inflammatory marker expression in PD macrophages upon T2DM, conforming to the properties of MS4A6A<sup>+</sup> macrophages [75].

Given that nearly 20 % of NASH patients progress to hepatic cirrhosis and eventually hepatocellular carcinoma [76]. It is therefore important to inhibit liver fibrosis progression in NASH stage as there are no available therapies for cirrhosis [77]. Previous studies have demonstrated that increased polarization of liver macrophages toward the M2-phenotype in the progression from NAFLD to NASH in patients and that NAFLD mice lacking M2-type macrophages had prominently attenuated hepatic inflammation and steatosis [78,79]. Our immune infiltration results also indicated a higher level of M2-type macrophages in NASH samples, and the main expression of MS4A6A biomarker by specific cycling macrophages. The great significance of high heterogeneity and the plasticity of macrophages' subpopulations in NASH progression has been emphasized in previous works, such as the TREM2<sup>+</sup>/CD9<sup>+</sup> macrophages and CCR2 bone marrow-derived macrophages [80]. Macrophages are considered to be key players in NAFLD and increase in liver periportal region as an early-stage histological hallmark [81]. In addition, the presence of *porphyromonas gingivalis*-derived lipopolysaccharide leads to the immuno-tolerant phenotype of macrophages in NAFLD [82].

Compared to type 1 diabetes mellitus, the predominant immune cell type causing islet inflammation in T2DM is macrophages [40], which accumulate and are featured by prominent MHCII expression [36]. Recent studies have also pointed out a mixed continuum of M1/M2 polarization phenotypes in macrophages in T2DM islet inflammation than a simple polarization toward the M1 or M2 state [36]. Coincidentally, the MS4A6A gene was identified as a robust contributor to the aggravation of diabetic nephropathy [83,84].

Such a consistent systemic response toward tissue macrophage phenotypes indicated an important role of MS4A6A<sup>+</sup> macrophages in mediating and favoring their

immunological similarities. Other works supported this notion by indicating that local immune cell alterations could regulate circulating immune cells, therefore intervening with other disease [85]. For example, macrophages can function as the most robust innate immune cells connecting PD and Alzheimer's disease [86]. Modulating certain molecular receptors in macrophages helps ameliorate hepatic steatosis and insulin resistance [87,88]. In addition, developing drugs for macrophages has been proven to be an effective way to alleviate the disease severity of NAFLD upon T2DM [89]. Our work concluded fenretinide (FEN) as a potential therapeutic reagent upon NAFLD, T2DM and PD conditions. As a synthetic derivative of retinoic acid, fenretinide treatment could repress lipid-induced reductions in insulin-stimulated glucose uptake by restoring ceramide and retinol homeostasis in vivo, which ultimately protected insulin signaling to reduce liver triglycerides accumulation, liver steatosis degree, and improve glucose homeostasis [90,91]. Besides, multiple studies have proven that such

effects are mediated by its inhibition of macrophages' pro-inflammatory activities, like targeting macrophagic 17  $\beta$ -HSD7 to ameliorate NAFLD [92], reducing macrophages-derived inflammatory mediators [93], and regulating polarization of macrophages [94]. Furthermore, a work showed its inhibition of *Aggregatibacter actinomycetemcomitans*. (specific pathogen for aggressive PD)-caused ceramide synthesis in macrophages [95].

The above-mentioned capacities of FEN on regulating cellular biosynthesis processes, macrophages, the pathogens for aggressive periodontitis, along with its high-affinity with MS4A6A receptor proteins imply its potentials in alleviating these inflammatory diseases through multiple pathways.

In summary, unsimilar to prior studies focusing on a single disease, our study for the first-time integrated patients' transcriptome data of PD, NAFLD, and T2DM at the same time, and provided robust pathologic mediators for intervention upon such three interrelated pathologies. Nevertheless, little is known about the biological functions of MS4A6A<sup>+</sup> macrophages in these situations and targeting MS4A6A proteins expressed by macrophages remains an outstanding problem [96].

## 5. Limitations

The work contains certain limitations. For example, it would be better to perform in vivo experiments to further verify the

relationship between MS4A6A<sup>+</sup> macrophages

and these three pathologies. Besides, the predicted therapeutic reagent FEN requires further efforts to investigate its real efficacy. In addition, the fact that macrophages are highly-heterogeneous and plastic, as well as targeting tissue-specific subsets of macrophages to reshape their functions, warrant more future exploration.

## 6. Conclusion

Our work revealed that MS4A6A<sup>+</sup> macrophages could be the central mediators of PD, NAFLD and T2DM progression, indicating FEN as a potential therapeutic drug.

## Funding

None.

## Data availability

All datasets used in the current work were fully available in the NCBI GEO repository: [<https://www.ncbi.nlm.nih.gov/geo/>], with accession numbers: GSE10334, GSE16134, GSE76895, GSE76894, GSE164760, GSE63067.

## Ethics declaration

Review and/or approval by an ethics committee was not needed for this study because this is a retrospective observational work analyzing de-identified public data available from the online NCBI GEO database <https://www.ncbi.nlm.nih.gov/geo/>, involving no intervention/experiment.

## Consent to participate

Informed consent was not required for this study because of unavailability.

## CRedit authorship contribution statement

**Junhao Wu:** Visualization, Methodology, Data curation, Conceptualization, Writing – original draft. **Jinsheng Wang:** Writing – original draft, Data curation, Conceptualization. **Caihan Duan:** Writing – original draft. **Chaoqun Han:** Writing – review & editing, Supervision. **Xiaohua Hou:** Writing – review & editing, Supervision, Project administration.

## Declaration of competing interest

The authors declare that they have no known competing financial interests or personal relationships that could have appeared to influence the work reported in this paper.

## Acknowledgment

We would like to thank all contributors to the references and open datasets utilized in the present study.

## Appendix A. Supplementary data

Supplementary data to this article can be found online at <https://doi.org/10.1016/j.heliyon.2024.e29340>.

## References

- [1] E. Albuquerque-Souza, S.E. Sahingur, Periodontitis, chronic liver diseases, and the emerging oral-gut-liver axis, *Periodontol.* 2000 89 (1) (2022) 125–141.
- [2] J. Slots, Periodontitis: facts, fallacies and the future, *Periodontol.* 2000 75 (1) (2017) 7–23.
- [3] M.X. Chen, et al., Global, regional, and national burden of severe periodontitis, 1990-2019: an analysis of the Global Burden of Disease Study 2019, *J. Clin. Periodontol.* 48 (9) (2021) 1165–1188.
- [4] M. Hatasa, et al., Relationship between NAFLD and periodontal disease from the View of clinical and basic research, and immunological response, *Int. J. Mol. Sci.* 22 (7) (2021).
- [5] R. Kuraji, et al., Periodontal disease-related nonalcoholic fatty liver disease and nonalcoholic steatohepatitis: an emerging concept of oral-liver axis, *Periodontol.* 2000 87 (1) (2021) 204–240.

- [6] J. Helenius-Hietala, et al., Periodontitis is associated with incident chronic liver disease-A population-based cohort study, *Liver Int.* 39 (3) (2019) 583–591.
- [7] K. Kuroe, et al., Association between periodontitis and fibrotic progression of non-alcoholic fatty liver among Japanese adults, *J. Clin. Periodontol.* 48 (3) (2021) 368–377.
- [8] A.A. Akinkugbe, et al., Periodontitis and non-alcoholic fatty liver disease, a population-based cohort investigation in the study of health in pomerania, *J. Clin. Periodontol.* 44 (11) (2017) 1077–1087.
- [9] E. Widita, et al., Relationship between clinical periodontal parameters and changes in liver enzymes levels over an 8-year period in an elderly Japanese population, *J. Clin. Periodontol.* 45 (3) (2018) 311–321.
- [10] R. Komazaki, et al., Periodontal pathogenic bacteria, *Aggregatibacter actinomycetemcomitans* affect non-alcoholic fatty liver disease by altering gut microbiota and glucose metabolism, *Sci. Rep.* 7 (1) (2017) 13950.
- [11] M. Yoneda, et al., Involvement of a periodontal pathogen, *Porphyromonas gingivalis* on the pathogenesis of non-alcoholic fatty liver disease, *BMC Gastroenterol.* 12 (2012) 16.
- [12] Y. Kamata, et al., Efficacy and safety of PERIODontal treatment versus usual care for Nonalcoholic liver disease: protocol of the PERION multicenter, two-arm, open-label, randomized trial, *Trials* 21 (1) (2020) 291.
- [13] F. Graziani, et al., Nonsurgical and surgical treatment of periodontitis: how many options for one disease? *Periodontol.* 2000 75 (1) (2017) 152–188.
- [14] P.Z. Zimmet, et al., Diabetes: a 21st century challenge, *Lancet Diabetes Endocrinol.* 2 (1) (2014) 56–64.
- [15] GBD 2021 Diabetes Collaborators, Global regional National burden of diabetes from 1990 to 2021, with projections of prevalence to 2050: a systematic analysis for the Global Burden of Disease Study 2021, *Lancet* 402 (10397) (2023) 203–234.
- [16] E. Lalla, P.N. Papapanou, Diabetes mellitus and periodontitis: a tale of two common interrelated diseases, *Nat. Rev. Endocrinol.* 7 (12) (2011) 738–748.
- [17] J. Stöhr, et al., Bidirectional association between periodontal disease and diabetes mellitus: a systematic review and meta-analysis of cohort studies, *Sci. Rep.* 11 (1) (2021) 13686.
- [18] C.H. Lee, D.T. Lui, K.S. Lam, Non-alcoholic fatty liver disease and type 2 diabetes: an update, *J Diabetes Investig* 13 (6) (2022) 930–940.
- [19] L.A. Adams, et al., NAFLD as a risk factor for the development of diabetes and the metabolic syndrome: an eleven-year follow-up study, *Am. J. Gastroenterol.* 104 (4) (2009) 861–867.
- [20] K.G. Tolman, et al., Spectrum of liver disease in type 2 diabetes and management of patients with diabetes and liver disease, *Diabetes Care* 30 (3) (2007) 734–743.
- [21] Z.M. Younossi, et al., The global epidemiology of NAFLD and NASH in patients with type 2 diabetes: a systematic review and meta-analysis, *J. Hepatol.* 71 (4) (2019) 793–801.
- [22] Z.M. Younossi, et al., Global epidemiology of nonalcoholic fatty liver disease-Meta-analytic assessment of prevalence, incidence, and outcomes, *Hepatology* 64 (1) (2016) 73–84.
- [23] N. Chalasani, et al., The diagnosis and management of nonalcoholic fatty liver disease: practice guidance from the American Association for the Study of Liver Diseases, *Hepatology* 67 (1) (2018) 328–357.
- [24] E.K. Spengler, R. Loomba, Recommendations for diagnosis, referral for liver biopsy, and treatment of nonalcoholic fatty liver disease and nonalcoholic steatohepatitis, *Mayo Clin. Proc.* 90 (9) (2015) 1233–1246.
- [25] C. Estes, et al., Modeling NAFLD disease burden in China, France, Germany, Italy, Japan, Spain, United Kingdom, and United States for the period 2016–2030, *J. Hepatol.* 69 (4) (2018) 896–904.
- [26] X.J. Wang, H. Malhi, Nonalcoholic fatty liver disease, *Ann. Intern. Med.* 169 (9) (2018) Itc65–itc80.
- [27] N. Chalasani, et al., The diagnosis and management of non-alcoholic fatty liver disease: practice guideline by the American association for the study of liver diseases, American College of Gastroenterology, and the American gastroenterological association, *Hepatology* 55 (6) (2012) 2005–2023.
- [28] W. Alazawi, et al., Periodontitis is associated with significant hepatic fibrosis in patients with non-alcoholic fatty liver disease, *PLoS One* 12 (12) (2017) e0185902.
- [29] F. Qiao, et al., The association between missing teeth and non-alcoholic fatty liver disease in adults, *J. Clin. Periodontol.* 45 (8) (2018) 941–951.
- [30] G. Hajishengallis, Periodontitis: from microbial immune subversion to systemic inflammation, *Nat. Rev. Immunol.* 15 (1) (2015) 30–44.
- [31] H. Tilg, A.R. Moschen, M. Roden, NAFLD and diabetes mellitus, *Nat. Rev. Gastroenterol. Hepatol.* 14 (1) (2017) 32–42.
- [32] E.E. Powell, V.W. Wong, M. Rinella, Non-alcoholic fatty liver disease, *Lancet* 397 (10290) (2021) 2212–2224.
- [33] E.E. Canfora, et al., Gut microbial metabolites in obesity, NAFLD and T2DM, *Nat. Rev. Endocrinol.* 15 (5) (2019) 261–273.
- [34] A. Luong, et al., Periodontitis and diabetes mellitus co-morbidity: a molecular dialogue, *J. Oral Biosci.* 63 (4) (2021) 360–369.
- [35] Z. Lu, et al., The presence of periodontitis exacerbates non-alcoholic fatty liver disease via sphingolipid metabolism-associated insulin resistance and hepatic inflammation in mice with metabolic syndrome, *Int. J. Mol. Sci.* 24 (9) (2023).
- [36] J. Guo, W. Fu, Immune regulation of islet homeostasis and adaptation, *J. Mol. Cell Biol.* 12 (10) (2020) 764–774.
- [37] G. Xourafa, M. Korbacher, M. Roden, Inter-organ crosstalk during development and progression of type 2 diabetes mellitus, *Nat. Rev. Endocrinol.* 20 (1) (2024) 27–49.
- [38] F. Cordero, M. Botta, R.A. Calogero, Microarray data analysis and mining approaches, *Brief Funct Genomic Proteomic* 6 (4) (2007) 265–281.
- [39] A.L. Chu, et al., The power of single-cell analysis for the study of liver pathobiology, *Hepatology* 73 (1) (2021) 437–448.
- [40] W. Ying, et al., The role of macrophages in obesity-associated islet inflammation and  $\beta$ -cell abnormalities, *Nat. Rev. Endocrinol.* 16 (2) (2020) 81–90.
- [41] T. Barrett, et al., NCBI GEO: archive for functional genomics data sets—update, *Nucleic Acids Res.* 41 (Database issue) (2013) D991–D995.
- [42] E.K. Gustavsson, et al., ggtranscript: an R package for the visualization and interpretation of transcript isoforms using ggplot2, *Bioinformatics* 38 (15) (2022) 3844–3846.
- [43] Z. Gu, R. Eils, M. Schlesner, Complex heatmaps reveal patterns and correlations in multidimensional genomic data, *Bioinformatics* 32 (18) (2016) 2847–2849.
- [44] M.S. Cline, et al., Integration of biological networks and gene expression data using Cytoscape, *Nat. Protoc.* 2 (10) (2007) 2366–2382.
- [45] Z. Li, M.J. Sillanpää, Overview of LASSO-related penalized regression methods for quantitative trait mapping and genomic selection, *Theor. Appl. Genet.* 125 (3) (2012) 419–435.
- [46] S. Engebretsen, J. Bohlén, Statistical predictions with glmnet, *Clin Epigenetics* 11 (1) (2019) 123.
- [47] J. Tolles, W.J. Meurer, Logistic regression: relating patient characteristics to outcomes, *JAMA* 316 (5) (2016) 533–534.
- [48] M. Li, et al., DISCO: a database of deeply integrated human single-cell omics data, *Nucleic Acids Res.* 50 (D1) (2022) D596–d602.
- [49] Y. Liu, et al., CB-Dock2: improved protein-ligand blind docking by integrating cavity detection, docking and homologous template fitting, *Nucleic Acids Res.* 50 (W1) (2022) W159–w164.
- [50] H. Yki-Järvinen, Non-alcoholic fatty liver disease as a cause and a consequence of metabolic syndrome, *Lancet Diabetes Endocrinol.* 2 (11) (2014) 901–910.
- [51] A. Cekici, et al., Inflammatory and immune pathways in the pathogenesis of periodontal disease, *Periodontol.* 2000 64 (1) (2014) 57–80.
- [52] C. Atri, F.Z. Guerfali, D. Laouini, Role of human macrophage polarization in inflammation during infectious diseases, *Int. J. Mol. Sci.* 19 (6) (2018).
- [53] O.A. Gonzalez, et al., Gingival transcriptomic patterns of macrophage polarization during initiation, progression, and resolution of periodontitis, *Clin. Exp. Immunol.* 211 (3) (2023) 248–268.
- [54] A. Mantovani, et al., The chemokine system in diverse forms of macrophage activation and polarization, *Trends Immunol.* 25 (12) (2004) 677–686.
- [55] Y. Zhou, et al., CD4(+) T cell activation and inflammation in NASH-related fibrosis, *Front. Immunol.* 13 (2022) 967410.
- [56] S. Hasiakos, et al., Calcium signaling in T cells and chronic inflammatory disorders of the oral cavity, *J. Dent. Res.* 100 (7) (2021) 693–699.
- [57] H. Xu, et al., CCR2(+) macrophages promote orthodontic tooth movement and alveolar bone remodeling, *Front. Immunol.* 13 (2022) 835986.
- [58] I. Mattioli, A. Mantovani, M. Locati, The tetraspan MS4A family in homeostasis, immunity, and disease, *Trends Immunol.* 42 (9) (2021) 764–781.
- [59] R. Sanyal, et al., MS4A4A: a novel cell surface marker for M2 macrophages and plasma cells, *Immunol. Cell Biol.* 95 (7) (2017) 611–619.
- [60] R. Silva-Gomes, et al., Differential expression and regulation of MS4A family members in myeloid cells in physiological and pathological conditions, *J. Leukoc. Biol.* 111 (4) (2022) 817–836.

- [61] N.B. McNamara, et al., Microglia regulate central nervous system myelin growth and integrity, *Nature* 613 (7942) (2023) 120–129.
- [62] X. Yang, et al., Functional characterization of Alzheimer's disease genetic variants in microglia, *Nat. Genet.* 55 (10) (2023) 1735–1744.
- [63] A.M. Smith, et al., Diverse human astrocyte and microglial transcriptional responses to Alzheimer's pathology, *Acta Neuropathol.* 143 (1) (2022) 75–91.
- [64] J. Wang, et al., Characterizing cellular heterogeneity in fibrotic hypersensitivity pneumonitis by single-cell transcriptional analysis, *Cell Death Discov* 8 (1) (2022) 38.
- [65] C. Zhang, et al., MS4A6A is a new prognostic biomarker produced by macrophages in glioma patients, *Front. Immunol.* 13 (2022) 865020.
- [66] E. Azizi, et al., Single-cell map of diverse immune phenotypes in the breast tumor microenvironment, *Cell* 174 (5) (2018) 1293–1308.e36.
- [67] Y.W. Dai, W.M. Wang, X. Zhou, Development of a CD8(+) T cell-based molecular classification for predicting prognosis and heterogeneity in triple-negative breast cancer by integrated analysis of single-cell and bulk RNA-sequencing, *Heliyon* 9 (9) (2023) e19798.
- [68] G.A. Pizzurro, K. Miller-Jensen, Reframing macrophage diversity with network motifs, *Trends Immunol.* 44 (12) (2023) 965–970.
- [69] A. Almubarak, et al., Disruption of monocyte and macrophage homeostasis in periodontitis, *Front. Immunol.* 11 (2020) 330.
- [70] W. Zhang, et al., Study on the imbalance of M1/M2 macrophage polarization in severe chronic periodontitis, *Technol. Health Care* 31 (1) (2023) 117–124.
- [71] C. Garaicoa-Pazmino, et al., Characterization of macrophage polarization in periodontal disease, *J. Clin. Periodontol.* 46 (8) (2019) 830–839.
- [72] G. Richard, et al., Partial restoration of macrophage alteration from diet-induced obesity in response to *Porphyromonas gingivalis* infection, *PLoS One* 8 (7) (2013) e70320.
- [73] Y. Wang, et al., Orthodontic compression enhances macrophage M2 polarization via histone H3 hyperacetylation, *Int. J. Mol. Sci.* 24 (4) (2023).
- [74] O.A. Gonzalez, et al., Differential gene expression profiles reflecting macrophage polarization in aging and periodontitis gingival tissues, *Immunol. Invest.* 44 (7) (2015) 643–664.
- [75] P. Agrafioti, et al., Decoding the role of macrophages in periodontitis and type 2 diabetes using single-cell RNA-sequencing, *Faseb j* 36 (2) (2022) e22136.
- [76] A.C. Sheka, et al., Nonalcoholic steatohepatitis: a review, *JAMA* 323 (12) (2020) 1175–1183.
- [77] D.C. Rockey, P.D. Bell, J.A. Hill, Fibrosis—a common pathway to organ injury and failure, *N. Engl. J. Med.* 372 (12) (2015) 1138–1149.
- [78] Y. Cao, et al., Macrophages evoke autophagy of hepatic stellate cells to promote liver fibrosis in NAFLD mice via the PGE2/EP4 pathway, *Cell. Mol. Life Sci.* 79 (6) (2022) 303.
- [79] D.J. Westcott, et al., MGL1 promotes adipose tissue inflammation and insulin resistance by regulating 7/4hi monocytes in obesity, *J. Exp. Med.* 206 (13) (2009) 3143–3156.
- [80] J.J. Zhang, et al., Integrative network-based analysis on multiple Gene Expression Omnibus datasets identifies novel immune molecular markers implicated in non-alcoholic steatohepatitis, *Front. Endocrinol.* 14 (2023) 1115890.
- [81] M. Peiseler, et al., Immune mechanisms linking metabolic injury to inflammation and fibrosis in fatty liver disease - novel insights into cellular communication circuits, *J. Hepatol.* 77 (4) (2022) 1136–1160.
- [82] L. Guo, et al., Liver macrophages show an immunotolerance phenotype in nonalcoholic fatty liver combined with *Porphyromonas gingivalis*-lipopolysaccharide infection, *Hua xi kou qiang yi xue za zhi* 41 (4) (2023) 385–394.
- [83] X. Wang, et al., CD163 in macrophages: a potential biomarker for predicting the progression of diabetic nephropathy based on bioinformatics analysis, *Endocr., Metab. Immune Disord.: Drug Targets* 23 (3) (2023) 294–303.
- [84] M. Zeng, et al., Identification of key biomarkers in diabetic nephropathy via bioinformatic analysis, *J. Cell. Biochem.* 120 (5) (2019) 8676–8688.
- [85] R.A. Irwandi, et al., Circulating inflammatory cell profiling and periodontitis: a systematic review and meta-analysis, *J. Leukoc. Biol.* 111 (5) (2022) 1069–1096.
- [86] J. Jin, et al., Immune-related signature of periodontitis and Alzheimer's disease linkage, *Front. Genet.* 14 (2023) 1230245.
- [87] Y.Y. Zhang, et al., Deletion of macrophage mineralocorticoid receptor protects hepatic steatosis and insulin resistance through ER $\alpha$ /HGF/met pathway, *Diabetes* 66 (6) (2017) 1535–1547.
- [88] R. Menghini, et al., TIMP3 overexpression in macrophages protects from insulin resistance, adipose inflammation, and nonalcoholic fatty liver disease in mice, *Diabetes* 61 (2) (2012) 454–462.
- [89] M. Samsuzzaman, et al., Identification of a potent NAFLD drug candidate for controlling T2DM-mediated inflammation and secondary damage in vitro and in vivo, *Front. Pharmacol.* 13 (2022) 943879.
- [90] B.T. Bikman, et al., Fenretinide prevents lipid-induced insulin resistance by blocking ceramide biosynthesis, *J. Biol. Chem.* 287 (21) (2012) 17426–17437.
- [91] B. Chaurasia, et al., Targeting a ceramide double bond improves insulin resistance and hepatic steatosis, *Science* 365 (6451) (2019) 386–392.
- [92] X. Dong, et al., Targeting macrophagic 17 $\beta$ -HSD7 by fenretinide for the treatment of nonalcoholic fatty liver disease, *Acta Pharm. Sin. B* 13 (1) (2023) 142–156.
- [93] C. Lachance, et al., Fenretinide corrects the imbalance between omega-6 to omega-3 polyunsaturated fatty acids and inhibits macrophage inflammatory mediators via the ERK pathway, *PLoS One* 8 (9) (2013) e74875.
- [94] Y. Cao, et al., Fenretinide regulates macrophage polarization to protect against experimental colitis induced by dextran sulfate sodium, *Bioengineered* 12 (1) (2021) 151–161.
- [95] H. Yu, M. Valerio, J. Bielawski, Fenretinide inhibited de novo ceramide synthesis and proinflammatory cytokines induced by *Aggregatibacter actinomycetemcomitans*, *J. Lipid Res.* 54 (1) (2013) 189–201.
- [96] K. Bitting, et al., Identification of redundancy between human Fc $\epsilon$ RI $\beta$  and MS4A6A proteins points toward additional complex mechanisms for Fc $\epsilon$ RI trafficking and signaling, *Allergy* 78 (5) (2023) 1204–1217.

**Junhao Wu**, M.Sc. Division of Gastroenterology, Union Hospital, Tongji Medical College, Huazhong University of Science and Technology, 1277 Jiefang Avenue, Wuhan, Hubei Province, China, E-mail: m202175773@hust.edu.cn

**Jinsheng Wang**, M.D. Department of Gastroenterology, Sir Run Run Shaw Hospital, College of Medicine, Zhejiang University, 3 East Qingchun Road, Hangzhou, Zhejiang Province, China, E-mail: wangjinsheng@zju.edu.cn

**Caihan Duan**, Ph.D. Division of Gastroenterology, Union Hospital, Tongji Medical College, Huazhong University of Science and Technology, 1277 Jiefang Avenue, Wuhan, Hubei Province, China, E-mail: dchyouxiang@163.com